Pulmonary transcriptomic responses indicate a dual role of inflammation in pneumonia development and viral clearance during 2009 pandemic influenza infection

Raquel Almansa [1], **Pamela Martínez-Orellana** [2], **Lucía Rico** [1], **Verónica Iglesias** [1], **Alicia Ortega** [1], **Beatriz Vidaña** [3], **Jorge Martínez** [2,4], **Ana Expósito** [1], **María Montoya** [2,5], **Jesús F. Bermejo-Martin** [Corresp. 1]

[1] Laboratory of Biomedical Research in Sepsis (BIOSEPSIS), Hospital Clínico Universitario de Valladolid - IECSCYL, Valladolid, Spain

[2] Centre de Recerca en Sanitat Animal (CReSA), Universitat Autónoma de Barcelona-IRTA, Barcelona, Spain

[3] Pathology Department, Animal and Plant Health Agency (APHA), Surrey, United Kingdom

[4] Departament de Sanitat i Anatomia Animals, Universitat Autónoma de Barcelona, Barcelona, Spain

[5] African Swine Fever Virus Immunology group, The Pirbright Institute, Surrey, United Kingdom

Corresponding Author: Jesús F. Bermejo-Martin
Email address: jfbermejo@saludcastillayleon.es

Background: The interaction between influenza virus and the host response to infection clearly plays an important role in determining the outcome of infection. While much is known on the participation of inflammation on the pathogenesis of severe A (H1N1) pandemic 09-influenza virus, its role in the course of non-fatal pneumonia has not been fully addressed.

Methods: A systems biology approach was used to define gene expression profiles, histology and viral dynamics in the lungs of healthy immune-competent mice with pneumonia caused by a human influenza A (H1N1) pdm09 virus, which successfully resolved the infection.

Results: Viral infection activated a marked pro-inflammatory response at the lung level paralleling the emergence of histological changes. Cellular immune response and Cytokine Signaling were the two signaling pathway categories more representative of our analysis. This transcriptome response was associated to viral clearance, and its resolution was accompanied by resolution of histopathology.

Discussion: These findings suggest a dual role of pulmonary inflammation in viral clearance and development of pneumonia during non-fatal infection caused by the 2009 pandemic influenza virus. Understanding the dynamics of the host's transcriptomic and virological changes over the course of the infection caused by A (H1N1) pdm09 virus may help identifying the immune response profiles associated to an effective response against influenza virus.

Pulmonary transcriptomic responses indicate a dual role of inflammation in pneumonia development and viral clearance during 2009 pandemic influenza infection

Raquel Almansa [a], Pamela Martínez-Orellana [b], Lucía Rico [a], Verónica Iglesias [a], Alicia Ortega [a], Beatriz Vidaña[c], Jorge Martínez[b,d] , Ana Expósito [a] , María Montoya [b,e], Jesús F. Bermejo-Martin [a].

[a] Laboratory of Biomedical Research in Sepsis (BIOSEPSIS), Hospital Clínico Universitario de Valladolid - IECSCYL, Valladolid, Spain.

[b] Centre de Recerca en Sanitat Animal (CReSA), Universitat Autónoma de Barcelona-IRTA, Barcelona, Spain.

[c] Pathology Department, Animal and Plant Health Agency (APHA), Surrey, United Kingdom.

[d] Departament de Sanitat i Anatomia Animals, Universitat Autónoma de Barcelona, Barcelona, Spain.

[e] African Swine Fever Virus Immunology group, The Pirbright Institute, Surrey, United Kingdom.

Corresponding author: Jesús F Bermejo-Martin. Grupo de Investigación Clínica en Infección Inmunidad y Genómica (ICIGEN), Hospital Clínico Universitario de Valladolid - IECSCYL, Av. Ramón y Cajal, 3, 47003 Valladolid, Spain. E-mail address: jfbermejo@saludcastillayleon.es.

Abstract

Background: The interaction between influenza virus and the host response to infection clearly plays an important role in determining the outcome of infection. While much is known on the participation of inflammation on the pathogenesis of severe A (H1N1) pandemic 09-influenza virus, its role in the course of non-fatal pneumonia has not been fully addressed.

Methods: A systems biology approach was used to define gene expression profiles, histology and viral dynamics in the lungs of healthy immune-competent mice with pneumonia caused by a human influenza A (H1N1) pdm09 virus, which successfully resolved the infection.

Results: Viral infection activated a marked pro-inflammatory response at the lung level paralleling the emergence of histological changes. Cellular immune response and Cytokine Signaling were the two signaling pathway categories more representative of our analysis. This transcriptome response was associated to viral clearance, and its resolution was accompanied by resolution of histopathology.

Discussion: These findings suggest a dual role of pulmonary inflammation in viral clearance and development of pneumonia during non-fatal infection caused by the 2009 pandemic influenza virus. Understanding the dynamics of the host's transcriptomic and virological changes over the course of the infection caused by A (H1N1) pdm09 virus may help identifying the immune response profiles associated to an effective response against influenza virus.

Introduction

Influenza is one of the most common respiratory infectious diseases and a worldwide public health concern. The World Health Organization (WHO) estimates that influenza viruses infect around 5%–15% of the global population, resulting into 250,000 to 500,000 deaths each year. (Vemula et al., 2016).

At the beginning of 2009, a new influenza virus of the subtype H1N1, [A (H1N1) pmd09], was detected in Mexico. The vast majority of infections caused by this new strain were mild and self-limiting upper respiratory tract illness. However, a small percentage of patients infected by the A H1N1 pm09 virus developed primary viral pneumonia, resulting in respiratory failure, acute respiratory distress, multi-organ failure and death (Health Protection Agency et al., 2009). A large proportion of these severe cases occurred in young adults with accompanying co-morbidities (chronic respiratory disease, cardiovascular disease, hypertension, obesity and diabetes) (Jain et al., 2009).

The host response to the infection clearly plays an important role in determining the outcome of the patients infected by influenza viruses (Almansa, Bermejo-Martín & de Lejarazu Leonardo, 2012). In this regard, severely infected patients by the influenza A (H1N1) pdm09 virus was characterized by the presence of high plasmatic levels of cytokines, chemokines and other immune mediators accompanying the presence of pneumonic infiltrates (Bermejo-Martin et al., 2009), (Hagau et al., 2010), (To et al., 2010). Moreover, we have shown that systemic levels of these mediators were directly associated with viral levels secreted by the respiratory tract from the beginning of the disease (Almansa et al., 2011a). In addition, persistence of viral secretion has been found in the patients with the worst outcomes (Lee et al., 2009), paralleling the presence of impaired expression of a number of genes participating in adaptive immune

responses. Depression of adaptive immunity response has been previouslycorrelated with poor control of infection and maintenance of inflammation, and secondarily with the generation of damage to the infected tissues with the development of further respiratory failure (Bermejo-Martin et al., 2010).

While much is known about the immune alterations and the participation of inflammation on the pathogenesis of severe A (H1N1) pandemic influenza, their role in the course of non-fatal pneumonia has not been sufficiently studied. Aimed to clarify this role, we employed a systems biology approach to study gene expression profiles and its relation to histology and viral dynamics in the lungs of healthy immune-competent mice with pneumonia caused by human influenza A (H1N1) pdm09 virus, which successfully resolved the infection.

Material and methods

Ethics statement

The ethical protocol and the research were reviewed and approved by the Animal and human Experimentation Ethical Committee of the Autonomous University of Barcelona (Internal Register Number 1124M2R) and the Ethical Animal Experimentation Commission of the Catalan Government (Register Number: 5767).

All the animal experiments were done at the Biosafety level 3 (BSL3) facilities of the Centre de Recerca en Sanitat Animal (CReSA, Barcelona, Spain). Animal care was performed according to the standard procedures of the center (Martínez-Orellana et al., 2015). Seven weeks-old C57BL6/JOlaHsd (C57BL6) female mice (Harlan Laboratories, Barcelona, Spain) were housed in groups in experimental isolation cages for one week in acclimation (72 animals in total). Throughout the experiment, all mice were provided with commercial food pellets and tap water *ad libitum.*

A (H1N1) pdm 2009 Catalonian virus and mice infection.

A human pandemic Influenza A virus, A/Catalonia/63/2009 (CAT09) (GenBank accession numbers GQ464405-GQ464411 and GQ168897) was used for animal infection (Busquets et al., 2010). CAT09 was passaged in MDCK two times and the viral stock had a titer of 106 PFU/ml. Animals were divided into two groups of 32 mice each; distribution was done as follows: untreated control group (mock group) and pdmH1N1 2009 infected-group (CAT09). To evaluate the pathogenicity mice were infected through intranasal instillation with 50 μL CAT09 at 104 PFU/mice as described previously (Itoh et al., 2009). Successful CAT09 mice infection and pathogenicity was previously confirmed by our experimental work (Orellana-Martínez,

2014). Control non-infected mice were treated with 50 µL phosphate-buffered saline (mock infection) to reproduce CAT09 infection.

Mice monitoring and sampling

During ten days, mice were observed daily to record changes in body weight and clinical signs. Based on our previous experimental work, the day showing the most important histological changes in the lung following infection caused by CAT09 is day 5, while resolution of histological changes occurs by day 10. Consistently with our previous experience (Orellana-Martínez, 2014), necropsies of 12 animals per group were performed at days 1, 5 and 10 post infection (dpi). Animals were euthanized with intraperitoneal inoculation of penthobarbital under anesthesia with 5% isofluprane and tissue samples of lung were dissected from dead animals using the standard surgical procedures. Lung samples of six animals per group were used for viral load determination and histological examination. Lung samples were snap frozen on dry ice and stored at –80°C until further processing. Gene expression profiling was performed for whole lungs of the other six animals per group by using microarrays.

Determination of viral load

Viral quantification was determined by plaque assay determining Plaque forming units (PFU) following our laboratory standard operating procedures (Martínez-Orellana et al., 2015). Briefly, supernatants were obtained after weighing, homogenizing and centrifuging lung samples. 0.1 ml of 10-fold supernatant dilutions were incubated with MDCK cells plated in 12-well tissue cultures plates for 1 hour. Then, cells were washed with phosphate buffer saline and plates were overlaid with 1.4% noble agar (Becton Dickinson, France), mixed 1:1 with 0.5 µg/ml of bovine trypsin and Minimum essential medium eagle (MEM) (both of Sigma-Aldrich SA, Madrid, Spain) supplemented with 100 UI/ml penicillin and 100ug/ml streptomycin (Invitrogen ®,

Barcelona, Spain). After 4 days of incubation, cells were fixed for 20 min using 10% formalin (Sigma-Aldrich SA, Madrid, Spain) and then overlaid with 1% crystal violet (Anorsa, Barcelona, Spain). Finally, cells were washed with water in order to visualized plaques, which were counted and compared to uninfected cells.

Histopathology

Lung samples were collected for macroscopical and histological examination according to our laboratory standard operating procedures (Martínez-Orellana et al., 2015). The procedures involved lung sample fixation using neutral-buffered 10% formalin for 48 hours, followed by embedment in paraffin wax. Next, sections of 3 μm were stained using haematoxylin and eosin (HE). Cross sections of the lungs were analysed separately. A semi-quantitative assessment of IAV-associated microscopic lesions in the lungs was performed for each animal. The lesional scoring was graded on the basis of lesion severity as previously described by Vidaña et al (Vidaña et al., 2014).

RNA extraction and microarray processing and analyzing

At designated time points (1, 5 and 10 dpi), C57BL6 mice were euthanized and lung tissue was collected in RNA-later and stored at –80°C until further processing. Total RNA was extracted from lung samples using the Ribopure kit (Ambion, Life technology). RNA integrity and concentration were evaluated as previously described (Almansa et al., 2015). A total amount of 100 ng of mRNA was processed as described to obtain Cyanine 3-CTP-labeled cRNA (Almansa et al., 2015). Next cRNA was hybridized with Mouse GE 4x44K v2 Microarray Kit (Agilent p/n G4846A) overnight (17hrs) at 65C on a rotator. Image acquisition was performed using an Agilent Microarray Scanner (Agilent G2565CA) and data were extracted using the Agilent Feature Extraction Software 10.7.1.1 following the Agilent protocol GE1-107_Sep09. Raw data

144 were collected and preprocessed by using the GeneSpring GX 12.0 software (Almansa et al.,
145 2015). This software was employed also to perform the statistical analysis, which involved the
146 use of a moderate T test to identify those genes showing significant differences between their
147 expression levels fixing a p-value < 0.05 with further application of the Benjamini-Hochberg
148 correction for multiple comparisons. A fold change in gene expression ≥ 2 was used to obtain the
149 list of those genes showing the more important variations in their expression levels between
150 groups along time (1, 5 and 10 dpi). Ingenuity pathway analysis (IPA) (Ingenuity Systems-
151 Quiagen, Redwood City, CA) was employed to determine whether a canonical pathway is
152 enriched with genes of interest by using Fisher's exact test.

153 ***Microarray Data Accession Number.***

154 Microarray expression data sets were uploaded at the Array Express microarray data repository
155 and are available publicly under accession number E-MTAB-3866.

156 ***Validation of gene expression results from microarrays.***

157 Results of gene expression obtained using microarrays were confirmed by using a next
158 generation PCR technology, droplet digital PCR (ddPCR), using the Bio-Rad QX200 ™ Droplet
159 Digital ™ PCR system. 5ng of total mRNA were retro-transcribed to cDNA and analysed by
160 ddPCR using a Bio-Rad QX200 ™ platform as previously described (Tamayo et al., 2014).
161 Quantification of expression levels of target mRNAs was performed using pre-designed
162 TaqMan® Assay Primer/Probe Sets, (FAM labelled MGB probes, Thermo Fisher/Scientific- Life
163 Technologies, Waltham, MA, USA): IL6 gene; interleukin 6 (Reference: Mm00446190_m1) and
164 IFNB1 gene; interferon beta 1 (Reference: Mm00439552_s1). The droplet reader used at least
165 10000 droplets to determine the percentage of positive droplets and calculation of copy number

166 of cDNA per ng of initial mRNA. Spearman correlation between ddPRC and microarrays results
167 was performed using SPSS 15.0. (Fig. S1).

168 ***Statistical analysis***

169 SPSS 15.00 software was employed for perform statistical comparison of weight loss and viral
170 load between groups at all sampling times (SPSS Inc., Chicago, IL, USA). The statistical test
171 used was the U Mann-Whitney, and the significance level (α) was set at 0.05. All graphs used for
172 represent the variations on weight loss and viral load were performed using GraphPad Prism 6
173 (GraphPad Software, La Jolla, CA, USA).

Results

A (H1N1) pdm09 virus infection induced moderate weight loss during the first five days of infection.

Weight was evaluated each day during the first 10 days following infection with the pandemic CAT09 virus. Even though the percentage of body weight loss in CAT09-infected animals was not dramatic, CAT09-infected mice showed significantly greater weight loss on the first five days compared to uninfected controls ($p < 0.05$). After 5 dpi, infected mice began to recover their normal weight with no significant differences compared to mock mice (Figure 1a).

Human A (H1N1) pdm09 virus causes a productive infection in the lower respiratory tract of mice.

Virus titers in lung homogenates measured on 1, 5 and 10 dpi are shown in Figure 1b (n= 6 mice per group). The highest value in viral load detected was one day after infection (average: 1.08E+05 PFU/g, SD: 1.43E+05). However, day 5 pi, infected animals were still secreting virus in lungs [1.01E+04 PFU/g, 0.86E+04], becoming undetectable at day 10 p.i.

CAT09-infected mice developed pneumonia at day 5 post-infection, fully recovering at day 10 post infection.

Lung tissues from 6 animals per group were histopathologically examined at day 1, 5 and 10 pi. As expected, control animals showed no histopathological lesions (Figure 2). Microscopic lesional scores were assigned for each animal (Figure 2 B). At 1 dpi, three of six infected mice presented histopathological lesions, two of them exhibited necrotizing bronchiolitis and the other one presented bronchointerstitial pneumonia. At day 5 pi, five of six animals presented severe bronchointerstitial pneumonia consisting of moderate to high numbers of lymphoplasmacytic cells and neutrophils infiltrated the bronchiole and surrounding alveoli (Figure 2). Nevertheless,

198 day 10 pi was characterized by the total resolution of lung lesions in the CAT09-infected
199 animals.

200 ***A (H1N1) pdm09 virus induced changes in gene expression levels in the lungs***

201 Gene expression profiles (GEP) at lungs were compared between six infected animals and six
202 mock mice at days 1, 5 and 10 pi. No differences in GEP were found at day 1 pi (Figure 3a), but
203 important differences were observed at day 5 pi, paralleling the development of histological
204 pneumonia (Figure 3b and Table S1). In the CAT09-infected mice group, 1264 genes showed a
205 significant variation of their expression levels by day 5 pi compared to the control group (418
206 up-regulated and 847 down expressed) (Figure 3b and Table S1). Genes showing the most
207 important differences between both groups were interleukin 6 (IL6) (Fold change FC: 86.6),
208 interferon beta 1 (IFNb) (FC: 62.6) and chemokine (C-X-C motif) ligand 10 (IP10), (FC: 43.3)
209 (Figure 3 e,f and Table S1). Expression levels of the vast majority of genes normalized by day
210 10, coinciding with virus clearance and resolution of histological changes (Figure 3 c, e, f and
211 Table S1). Only 30 out of the 1264 genes kept on showing altered expression levels by day 10 p.i
212 (Figure S2 and Table S1). Interestingly, expression levels of IL6 persisted remarkably high by
213 this time point (FC:10.91) along with those of granzyme K (Gzmk) (FC:15.8) (Figure S2).

214 ***A (H1N1) pdm09 infection turned on the expression of genes involved in the innate response***
215 ***and in the switch to adaptive immunity by day 5 pi.***

216 Since most differences in gene expression were found by day 5 pi, we focused the Ingenuity
217 pathway analysis (IPA) on that day. The list of 1264 genes (either up and down regulated) was
218 analyzed by IPA in order to identify the canonical pathways that were enriched at day 5 pi.
219 Notably, Cellular immune response and Cytokine Signaling were the two signaling pathway

220 categories more representative of our analysis (Table S2). The most significant canonical
221 pathways identify by IPA are describe in table 1 and figure 3d.
222 Most of these pathways were involved in the innate immune response and inflammation: [Role
223 of Hypercytokinemia/ hyperchemokinemia in the Pathogenesis of Influenza (Figure 4), Hepatic
224 Fibrosis/Hepatic Stellate Cell Activation, Agranulocyte Adhesion and Diapedesis, TREM1
225 Signaling, Differential Regulation of Cytokine Production in Intestinal Epithelial Cells by IL-
226 17A and IL-17F, Granulocyte Adhesion and Diapedesis, Altered T Cell and B Cell Signaling in
227 Rheumatoid Arthritis, Differential Regulation of Cytokine Production in Macrophages and T
228 Helper Cells by IL-17A and IL-17F, Role of IL-17F in Allergic Inflammatory Airway Diseases,
229 Graft-versus-Host Disease Signaling, Role of Macrophages, Fibroblasts and Endothelial Cells in
230 Rheumatoid Arthritis, Role of Pattern Recognition Receptors in Recognition of Bacteria and
231 Viruses and Wnt/β-catenin Signaling pathway]. The vast majority of the genes involved in these
232 pathways coded for cytokines (Table S2). H1N1 virus also induced alterations in pathways
233 participating in the switch from innate to adaptive immunity: [Communication between Innate
234 and Adaptive Immune Cells, Crosstalk between Dendritic Cells and Natural Killer Cells, T
235 Helper Cell Differentiation]. Supplementary table S3 and figure 3 e,f show the variation of the
236 genes participating in these pathways along the study course.
237

239 **Discussion**

240 The overarching aim of this work was to study the role of inflammation at pulmonary level
241 during a non-fatal infection caused by the 2009 pandemic influenza virus using the mice model.
242 In this sense, we analyzed the gene expression profiles (GEP) and its relation to histology and
243 viral dynamics in the lungs of healthy immune-competent mice with pneumonia caused by
244 human influenza A (H1N1) pdm09 virus.

245 Our GEP analysis allowed us to identify the presence of marked activation of innate immunity
246 genes by day 5post infection, paralleling the existence of extensive pneumonic/cellular infiltrates
247 in the lung, and active viral replication. The innate immune response is the first line of defence
248 against invading viruses (Iwasaki & Pillai, 2014). Infection of the respiratory tract induced thus a
249 typical antiviral response characterised by the activation of pro-inflammatory cytokines and
250 interferon (IFNs) response genes (ISGs). In our analysis, the genes showing higher differences
251 for their expression levels between infected mice and controls were IL6, IFNb, and IP10. These
252 molecules, along with TNF and IL1b (also over-expressed at day 5), are the major cytokines
253 limiting viral replication during influenza infection, recruiting immune cells to the sites of
254 infection and producing inflammation (Nicholls, 2013).

255 IL6 is a pro-inflammatory cytokine which role in the pathogenesis of the A (H1N1) pdm09
256 remains unclear. There is a consensus in the literature about the existence of high systemic levels
257 of IL6 in severe patients infected by A (H1N1) pdm09 virus (Bermejo-Martin et al., 2009) (To et
258 al., 2010) (Zúñiga et al., 2011). This molecule induces pro-inflammatory responses such as
259 leukocyte recruitment into the lung. Excessive production of IL6 has been associated with
260 several pathological manifestations(Ho, Luo & Lai, 2015) (Baillet et al., 2015). However,
261 Paquette et al demonstrated in IL6 deficient mice infected with A (H1N1) pdm09, that no

262 significant differences in survival, weight loss, viral load, or pathology were observed between
263 IL6 deficient and wild-type mice following infection. Based in our results, presence of high
264 expression levels of this cytokine in the lung at day 10 could indicate that this cytokine plays a
265 role in viral clearance and tissue repair after pneumonia. Other mouse models support the idea of
266 a protective role of IL6 in influenza infections (Lauder et al., 2013).
267 IFNb is a cytokine member of type I interferon family. It induces an antiviral state in infected
268 and neighbouring cells (Ramos & Fernandez-Sesma, 2015). To do so, IFNs induce the
269 transcription of hundreds of ISGs, which leads to numerous changes in the transcriptome of the
270 cell. Interestingly, in our analysis, some OAS genes (OAS1a, OAS1f, OASL1 and OAS2), IFIT
271 genes (IFIT1, IFIT2 and IFIT3), MX1, SOCS1 and CXCL10, all of them IGS genes, showed
272 high expression levels in the infected mice compared with controls. The antiviral interferon
273 response increased at day 5 pi. but decreased at day 10 pi. coinciding whit viral clearance. These
274 results are similar to the observations reported in previous studies using ferrets infected by A
275 (H1N1) pdm09 virus (León et al., 2013) (Rowe et al., 2010b). This authors showed an early
276 robust innate ISG and chemokine response that shut down on day 7-10 pi, when viral load was
277 undetectable.
278 The activation of a group of genes involved in the "Role of
279 hypercytokinemia/hyperchemokinemia in the Pathogenesis of Influenza" pathway, evidence the
280 existence of a local "cytokine storm" in the lung, following infection by A (H1N1) pdm09 virus.
281 Hypercytokinemia/hyperchemokinemia is a common finding that characterized an influenza
282 infection at transcriptomic level (Morrison et al., 2014), (Ma et al., 2011), (León et al., 2013),
283 (Rowe et al., 2010b) . Several experimental studies suggested that cytokine storm correlated
284 directly with tissue injury and an unfavorable prognosis of severe influenza (Liu, Zhou & Yang,

2016). In our study, concomitant with high expression levels of IL6, IFNb and ISGs, the virus activated Th1 and chemokine responses mediated by IL1a, IL1b, IL12b,TNF, MCP1 and RANTES. These results are similar to those found at systemic level in patients with primary viral pneumonia (Bermejo-Martin et al., 2009) (Hagau et al., 2010) (To et al., 2010). In our model, the marked inflammatory program observed by day 5 in the lung got deactivated by day 10, paralleling resolution of histological changes and viral replication. Moreover, evaluation of gene expression levels along time in the infected group confirmed the appearance of a strong pro-inflammatory response at day 5 that is downmodulated at day 10 (Figure 3e,f and Supplementary table S3). Similar results were also found in other experimental studies (Josset et al., 2012b), (León et al., 2013), (Rowe et al., 2010b), where the decreased of cytokine expression levels characterized the recovery phase of the disease. Therefore, a failure to effectively regulation of excessive inflammation may be, in part, responsible for severe cases of 2009-H1N1.

In turn, the activation of genes involved in "Agranulocyte Adhesion and Diapedesis", "TREM1 Signaling", "Granulocyte Adhesion and Diapedesis", "Graft-versus-Host Disease Signaling and "Role of Pattern Recognition Receptors in Recognition of Bacteria and Viruses" might confirm the existence of a transcriptomic program aimed to recruit lymphocytes, monocytes and neutrophils to the site of infection. Histological studies at day 5 pi confirmed the presence of extensive pneumonic/cellular infiltrates into the lung. Although the primary role of the innate immune response is limiting viral replication, excessive activation of innate immunity could induce tissue damage (Vidaña et al., 2014) (de Jong et al., 2006). This phenomenon seems to occur also in the context of autoimmunity diseases such as Rheumatoid Arthritis (Catrina et al., 2016). In fact, "Altered T Cell and B Cell Signaling in Rheumatoid Arthritis" and "Role of Macrophages, Fibroblasts and Endothelial Cells in Rheumatoid Arthritis" are two of the

significant pathways identified by IPA in our analysis. In influenza disease, an exaggerated inflammatory response has been cited as the cause of pulmonary oedema, alveolar haemorrhage and acute respiratory distress syndrome, conditions associated with necrosis and tissue destruction (To et al., 2001). Most of the genes participating in these pathways decreased their expression levels on day 10 pi. paralleling resolution of pneumonia, reinforcing the idea that a correct modulation of inflammatory response is essential for recovery in this disease.

IPA identified also three pathways related to interleukin 17: "Differential Regulation of Cytokine Production in Intestinal Epithelial Cells by IL-17A and IL-17F, "Differential Regulation of Cytokine Production in Macrophages and T Helper Cells by IL-17A and IL-17F and "Role of IL-17F in Allergic Inflammatory Airway Diseases". Th-17 immunity participates in clearing pathogens during host defence reactions but is involved also in tissue inflammation in several autoimmune diseases, allergic diseases, and asthma (Nalbandian, Crispín & Tsokos, 2009) (Cheung, Wong & Lam, 2008). In severe influenza it has been proposed to play a beneficial role (Iwakura et al., 2008) (Bermejo-Martin et al., 2009) (Almansa et al., 2011b).

IPA also identified low expression levels of a group of genes involved in the "Wnt/β-catenin Signaling pathway" at 5 pi. It has been previously described that influenza virus down-regulates the expression of proteins of this pathway like FZD (Shapira et al., 2009). This is consistent with low expression levels of FZD2 and FZD7 genes found in our analysis. The biological repercussion associated to down-modulation of this pathway remains to be elucidated.

Finally, the activation of those cytokine genes involved in the [Communication between Innate and Adaptive Immune Cells, Crosstalk between Dendritic Cells and Natural Killer Cells, T Helper Cell Differentiation] signalling pathways at day 5 pi. could be reflecting the development of the adaptive immune response against the virus. Later

activation of the adaptive immune response was previously supported by increased levels of granzyme mRNAs in blood cells (Rowe et al., 2010a). In our study, the virus induced the expression of granzyme A, B, and K at day 5 pi. Moreover, expression levels of gramzyme K persisted remarkably high at day 10 pi, which is consistent with the data published in ferret infected by A (H1N1) pdm09 virus (Rowe et al., 2010a).

There are several works evaluating host transcriptomic responses to A (H1N1) pdm09 virus using animal models (Powell & Waters, 2017) , with different scope, but not of all them properly integrate the gene expression profiles induced by the infection with the pathogenic events to built a comprehensive model to improve our understanding on the events underlying the appearance and resolution of pneumonia caused by influenza (see table S4). The vast majority of these experimental models have focused on studying the host immune responses to the virus only on the acute phase of infection (Ma et al., 2011), (Camp et al., 2012), (Josset et al., 2012a), (Zou et al., 2013), (Morrison et al., 2014). The present work studies the relationship between host transcriptomic responses and the progression and resolution of infection caused by the A (H1N1) pdm09 influenza virus. The most similar study to the one we present here is that published by Rowe et al, 2010. In that paper, the authors employ ferrets, which is one of the best models to reproduce human pathology in the context of influenza but, at the same time it is not an easily available model, being expensive and complicated to manage. Our study employed a mouse model, which is a more affordable, but nonetheless reproduced the major findings of Rowe *et al*, who evidenced the existence of a exuberant cytokine and chemokines response at the lungs paralleling histological changes, which was down-modulated following resolution of these changes (Rowe et al., 2010b). Our results support thus the potential use of this mice model for the study of immunopathology in influenza infection and for those works evaluating

immunomodulators for the treatment of this disease. While other studies uses a mice adapted influenza strain such as PR8 (Pommerenke et al., 2012) or other mouse passaged 2009 strains, (Josset et al., 2012a), (Manchanda et al., 2016), our study employs a strain obtained directly form a human patient. Mouse adaptation results in increased virulence and lung pathology and also induces a strong host transcriptional response after infection compared with non adapted influenza strains (Josset et al., 2012a). In our opinion, our model could help to better understand the immune-pathogenic events on the basis of the most common scenario during the pandemics, which was that corresponding to a non severe infection.

Conclusions

In conclusion, our findings suggest a dual role of pulmonary inflammation during non-fatal infection caused by the 2009 pandemic influenza virus. On one side, the activation in the lung of a marked innate immunity transcriptomic program was associated to the appearance of pneumonia, but on the other hand, activation of this program paralleled viral clearance (Figure 5). Understanding the dynamics of the host's transcriptomic and virus changes over the course of the infection caused by A (H1N1) pdm09 might help to identify the immune response profiles associated to effective / balanced responses against influenza virus.

Acknowledgments:

The authors kindly thank to the BSL3 facility staff for the technical support they provided during the experimental infection period. The authors are also grateful to Dr Tomas Pumarola's laboratory from Hospital Clinic of Barcelona in Spain, for the generous gift of human pandemic Influenza A virus, A/Catalonia/63/2009.

References:

Almansa R., Anton A., Ramirez P., Martin-Loeches I., Banner D., Pumarola T., Xu L., Blanco J., Ran L., Lopez-Campos G., Martin-Sanchez F., Socias L., Loza A., Andaluz D., Maravi E., Gordón M., Gallegos MC., Fernandez V., León C., Merino P., Marcos MA., Gandía F., Bobillo F., Resino S., Eiros JM., Castro C., Mateo P., Gonzalez-Rivera M., Rello J., de Lejarazu RO., Kelvin DJ., Bermejo-Martin JF. 2011a. Direct association between pharyngeal viral secretion and host cytokine response in severe pandemic influenza. *BMC infectious diseases* 11:232. DOI: 10.1186/1471-2334-11-232.

Almansa R., Bermejo-Martín JF., de Lejarazu Leonardo RO. 2012. Immunopathogenesis of 2009 pandemic influenza. *Enfermedades Infecciosas Y Microbiología Clínica* 30 Suppl 4:18–24. DOI: 10.1016/S0213-005X(12)70100-3.

Almansa R., Heredia-Rodríguez M., Gomez-Sanchez E., Andaluz-Ojeda D., Iglesias V., Rico L., Ortega A., Gomez-Pesquera E., Liu P., Aragón M., Eiros JM., Jiménez-Sousa MÁ., Resino S., Gómez-Herreras I., Bermejo-Martín JF., Tamayo E. 2015. Transcriptomic correlates of organ failure extent in sepsis. *The Journal of Infection* 70:445–456. DOI: 10.1016/j.jinf.2014.12.010.

Almansa R., Socias L., Ramirez P., Martin-Loeches I., Vallés J., Loza A., Rello J., Kelvin DJ., León C., Blanco J., Andaluz D., Micheloud D., Maraví E., Ortiz de Lejarazu R., Bermejo-Martin JF. 2011b. Imbalanced pro- and anti-Th17 responses (IL-17/granulocyte colony-stimulating factor) predict fatal outcome in 2009 pandemic influenza. *Critical Care (London, England)* 15:448. DOI: 10.1186/cc10426.

Baillet A., Gossec L., Paternotte S., Etcheto A., Combe B., Meyer O., Mariette X., Gottenberg J-E., Dougados M. 2015. Evaluation of Serum Interleukin-6 Level as a Surrogate Marker of Synovial Inflammation and as a Factor of Structural Progression in Early Rheumatoid Arthritis: Results From a French National Multicenter Cohort. *Arthritis Care & Research* 67:905–912. DOI: 10.1002/acr.22513.

Bermejo-Martin JF., Martin-Loeches I., Rello J., Antón A., Almansa R., Xu L., Lopez-Campos G., Pumarola T., Ran L., Ramirez P., Banner D., Ng DC., Socias L., Loza A., Andaluz D., Maravi E., Gómez-Sánchez MJ., Gordón M., Gallegos MC., Fernandez V., Aldunate S., León C., Merino P., Blanco J., Martin-Sanchez F., Rico L., Varillas D., Iglesias V., Marcos MÁ., Gandía F., Bobillo F., Nogueira B., Rojo S., Resino S., Castro C., Ortiz de Lejarazu R., Kelvin D. 2010. Host adaptive immunity deficiency in severe pandemic influenza. *Critical Care (London, England)* 14:R167. DOI: 10.1186/cc9259.

Bermejo-Martin JF., Ortiz de Lejarazu R., Pumarola T., Rello J., Almansa R., Ramírez P., Martin-Loeches I., Varillas D., Gallegos MC., Serón C., Micheloud D., Gomez JM., Tenorio-Abreu A., Ramos MJ., Molina ML., Huidobro S., Sanchez E., Gordón M., Fernández V., Del Castillo A., Marcos MA., Villanueva B., López CJ., Rodríguez-Domínguez M., Galan J-C., Cantón R., Lietor A., Rojo S., Eiros JM., Hinojosa C., Gonzalez I., Torner N., Banner D., Leon A., Cuesta P., Rowe T., Kelvin DJ. 2009. Th1 and Th17 hypercytokinemia as early host response signature in severe pandemic influenza. *Critical Care (London, England)* 13:R201. DOI: 10.1186/cc8208.

Busquets N., Segalés J., Córdoba L., Mussá T., Crisci E., Martín-Valls GE., Simon-Grifé M., Pérez-Simó M., Pérez-Maíllo M., Núñez JI., Abad FX., Fraile L., Pina S., Majó N., Bensaid A., Domingo M., Montoya M. 2010. Experimental infection with H1N1 European swine influenza virus protects pigs from an infection with the 2009 pandemic H1N1 human influenza virus. *Veterinary Research* 41:74. DOI: 10.1051/vetres/2010046.

Camp JV., Svensson TL., McBrayer A., Jonsson CB., Liljeström P., Bruder CE. 2012. De-novo transcriptome sequencing of a normalized cDNA pool from influenza infected ferrets. *PloS One* 7:e37104. DOI: 10.1371/journal.pone.0037104.

Catrina AI., Joshua V., Klareskog L., Malmström V. 2016. Mechanisms involved in triggering rheumatoid arthritis. *Immunological Reviews* 269:162–174. DOI: 10.1111/imr.12379.

Cheung PFY., Wong CK., Lam CWK. 2008. Molecular mechanisms of cytokine and chemokine release from eosinophils activated by IL-17A, IL-17F, and IL-23: implication for Th17 lymphocytes-mediated allergic inflammation. *Journal of Immunology (Baltimore, Md.: 1950)* 180:5625–5635.

Hagau N., Slavcovici A., Gonganau DN., Oltean S., Dirzu DS., Brezoszki ES., Maxim M., Ciuce C., Mlesnite M., Gavrus RL., Laslo C., Hagau R., Petrescu M., Studnicska DM. 2010. Clinical aspects and cytokine response in severe H1N1 influenza A virus infection. *Critical Care (London, England)* 14:R203. DOI: 10.1186/cc9324.

Health Protection Agency, Health Protection Scotland, National Public Health Service for Wales, HPA Northern Ireland Swine influenza investigation teams 2009. Epidemiology of new influenza A (H1N1) virus infection, United Kingdom, April-June 2009. *Euro Surveillance: Bulletin Européen Sur Les Maladies Transmissibles = European Communicable Disease Bulletin* 14.

Ho L-J., Luo S-F., Lai J-H. 2015. Biological effects of interleukin-6: Clinical applications in autoimmune diseases and cancers. *Biochemical Pharmacology* 97:16–26. DOI: 10.1016/j.bcp.2015.06.009.

Itoh Y., Shinya K., Kiso M., Watanabe T., Sakoda Y., Hatta M., Muramoto Y., Tamura D., Sakai-Tagawa Y., Noda T., Sakabe S., Imai M., Hatta Y., Watanabe S., Li C., Yamada S., Fujii K., Murakami S., Imai H., Kakugawa S., Ito M., Takano R., Iwatsuki-Horimoto K., Shimojima M., Horimoto T., Goto H., Takahashi K., Makino A., Ishigaki H., Nakayama M., Okamatsu M., Takahashi K., Warshauer D., Shult PA., Saito R., Suzuki H., Furuta Y., Yamashita M., Mitamura K., Nakano K., Nakamura M., Brockman-Schneider R., Mitamura H., Yamazaki M., Sugaya N., Suresh M., Ozawa M., Neumann G., Gern J., Kida H., Ogasawara K., Kawaoka Y. 2009. In vitro and in vivo characterization of new swine-origin H1N1 influenza viruses. *Nature* 460:1021–1025. DOI: 10.1038/nature08260.

Iwakura Y., Nakae S., Saijo S., Ishigame H. 2008. The roles of IL-17A in inflammatory immune responses and host defense against pathogens. *Immunological Reviews* 226:57–79. DOI: 10.1111/j.1600-065X.2008.00699.x.

Iwasaki A., Pillai PS. 2014. Innate immunity to influenza virus infection. *Nature Reviews. Immunology* 14:315–328. DOI: 10.1038/nri3665.

Jain S., Kamimoto L., Bramley AM., Schmitz AM., Benoit SR., Louie J., Sugerman DE., Druckenmiller JK., Ritger KA., Chugh R., Jasuja S., Deutscher M., Chen S., Walker JD., Duchin JS., Lett S., Soliva S., Wells EV., Swerdlow D., Uyeki TM., Fiore AE., Olsen SJ., Fry AM., Bridges CB., Finelli L., 2009 Pandemic Influenza A (H1N1) Virus Hospitalizations Investigation Team 2009. Hospitalized patients with 2009 H1N1 influenza in the United States, April-June 2009. *The New England Journal of Medicine* 361:1935–1944. DOI: 10.1056/NEJMoa0906695.

de Jong MD., Simmons CP., Thanh TT., Hien VM., Smith GJD., Chau TNB., Hoang DM., Van Vinh Chau N., Khanh TH., Dong VC., Qui PT., Van Cam B., Ha DQ., Guan Y., Peiris JSM., Chinh NT., Hien TT., Farrar J. 2006. Fatal outcome of human influenza A (H5N1) is associated with high viral load and hypercytokinemia. *Nature Medicine* 12:1203–1207. DOI: 10.1038/nm1477.

Josset L., Belser JA., Pantin-Jackwood MJ., Chang JH., Chang ST., Belisle SE., Tumpey TM., Katze MG. 2012a. Implication of inflammatory macrophages, nuclear receptors, and interferon regulatory factors in increased virulence of pandemic 2009 H1N1 influenza A virus after host adaptation. *Journal of Virology* 86:7192–7206. DOI: 10.1128/JVI.00563-12.

Josset L., Engelmann F., Haberthur K., Kelly S., Park B., Kawoaka Y., García-Sastre A., Katze MG., Messaoudi I. 2012b. Increased viral loads and exacerbated innate host responses in aged macaques infected with the 2009 pandemic H1N1 influenza A virus. *Journal of Virology* 86:11115–11127. DOI: 10.1128/JVI.01571-12.

Lauder SN., Jones E., Smart K., Bloom A., Williams AS., Hindley JP., Ondondo B., Taylor PR., Clement M., Fielding C., Godkin AJ., Jones SA., Gallimore AM. 2013. Interleukin-6 limits influenza-induced inflammation and protects against fatal lung pathology. *European Journal of Immunology* 43:2613–2625. DOI: 10.1002/eji.201243018.

Lee N., Chan PKS., Hui DSC., Rainer TH., Wong E., Choi K-W., Lui GCY., Wong BCK., Wong RYK., Lam W-Y., Chu IMT., Lai RWM., Cockram CS., Sung JJY. 2009. Viral loads and duration of viral shedding in adult patients hospitalized with influenza. *The Journal of Infectious Diseases* 200:492–500. DOI: 10.1086/600383.

León AJ., Banner D., Xu L., Ran L., Peng Z., Yi K., Chen C., Xu F., Huang J., Zhao Z., Lin Z., Huang SHS., Fang Y., Kelvin AA., Ross TM., Farooqui A., Kelvin DJ. 2013. Sequencing, annotation, and characterization of the influenza ferret infectome. *Journal of Virology* 87:1957–1966. DOI: 10.1128/JVI.02476-12.

Liu Q., Zhou Y., Yang Z. 2016. The cytokine storm of severe influenza and development of immunomodulatory therapy. *Cellular and Molecular Immunology* 13:3–10. DOI: 10.1038/cmi.2015.74.

Ma W., Belisle SE., Mosier D., Li X., Stigger-Rosser E., Liu Q., Qiao C., Elder J., Webby R.,

Katze MG., Richt JA. 2011. 2009 pandemic H1N1 influenza virus causes disease and upregulation of genes related to inflammatory and immune responses, cell death, and lipid metabolism in pigs. *Journal of Virology* 85:11626–11637. DOI: 10.1128/JVI.05705-11.

Manchanda H., Seidel N., Blaess MF., Claus RA., Linde J., Slevogt H., Sauerbrei A., Guthke R., Schmidtke M. 2016. Differential Biphasic Transcriptional Host Response Associated with Coevolution of Hemagglutinin Quasispecies of Influenza A Virus. *Frontiers in Microbiology* 7:1167. DOI: 10.3389/fmicb.2016.01167.

Martínez-Orellana P., Martorell J., Vidaña B., Majó N., Martínez J., Falcón A., Rodríguez-Frandsen A., Casas I., Pozo F., García-Migura L., García-Barreno B., Melero JA., Fraile L., Nieto A., Montoya M. 2015. Clinical response to pandemic h1n1 influenza virus from a fatal and mild case in ferrets. *Virology Journal* 12. DOI: 10.1186/s12985-015-0272-x.

Orellana-Martínez P. 2014. Analysis of host responses and fitness in different pandemic H1N1 (2009) influenza virus in mice and ferrets. Ph.D. Thesis. Universitat Autònoma de Barcelona.

Morrison J., Josset L., Tchitchek N., Chang J., Belser JA., Swayne DE., Pantin-Jackwood MJ., Tumpey TM., Katze MG. 2014. H7N9 and other pathogenic avian influenza viruses elicit a three-pronged transcriptomic signature that is reminiscent of 1918 influenza virus and is associated with lethal outcome in mice. *Journal of Virology* 88:10556–10568. DOI: 10.1128/JVI.00570-14.

Nalbandian A., Crispín JC., Tsokos GC. 2009. Interleukin-17 and systemic lupus erythematosus: current concepts. *Clinical and Experimental Immunology* 157:209–215. DOI: 10.1111/j.1365-2249.2009.03944.x.

Nicholls JM. 2013. The battle between influenza and the innate immune response in the human respiratory tract. *Infection & Chemotherapy* 45:11–21. DOI: 10.3947/ic.2013.45.1.11.

Pommerenke C., Wilk E., Srivastava B., Schulze A., Novoselova N., Geffers R., Schughart K. 2012. Global transcriptome analysis in influenza-infected mouse lungs reveals the kinetics of innate and adaptive host immune responses. *PloS One* 7:e41169. DOI: 10.1371/journal.pone.0041169.

Powell JD., Waters KM. 2017. Influenza-Omics and the Host Response: Recent Advances and Future Prospects. *Pathogens (Basel, Switzerland)* 6. DOI: 10.3390/pathogens6020025.

Ramos I., Fernandez-Sesma A. 2015. Modulating the Innate Immune Response to Influenza A Virus: Potential Therapeutic Use of Anti-Inflammatory Drugs. *Frontiers in Immunology* 6:361. DOI: 10.3389/fimmu.2015.00361.

Rowe T., Banner D., Farooqui A., Ng DCK., Kelvin AA., Rubino S., Huang SSH., Fang Y., Kelvin DJ. 2010a. In vivo ribavirin activity against severe pandemic H1N1 Influenza A/Mexico/4108/2009. *The Journal of General Virology* 91:2898–2906. DOI: 10.1099/vir.0.024323-0.

Rowe T., León AJ., Crevar CJ., Carter DM., Xu L., Ran L., Fang Y., Cameron CM., Cameron MJ., Banner D., Ng DC., Ran R., Weirback HK., Wiley CA., Kelvin DJ., Ross TM. 2010b. Modeling host responses in ferrets during A/California/07/2009 influenza infection. *Virology* 401:257–265. DOI: 10.1016/j.virol.2010.02.020.

Shapira SD., Gat-Viks I., Shum BOV., Dricot A., de Grace MM., Wu L., Gupta PB., Hao T., Silver SJ., Root DE., Hill DE., Regev A., Hacohen N. 2009. A Physical and Regulatory Map of Host-Influenza Interactions Reveals Pathways in H1N1 Infection. *Cell* 139:1255–1267. DOI: 10.1016/j.cell.2009.12.018.

Tamayo E., Almansa R., Carrasco E., Ávila-Alonso A., Rodríguez-Fernández A., Wain J., Heredia M., Gomez-Sanchez E., Soria S., Rico L., Iglesias V., Martínez-Martínez A., Andaluz-Ojeda D., Herreras JIG., Eiros JM., Bermejo-Martin JF. 2014. Quantification of IgM molecular response by droplet digital PCR as a potential tool for the early diagnosis of sepsis. *Critical Care (London, England)* 18:433. DOI: 10.1186/cc13910.

To KF., Chan PK., Chan KF., Lee WK., Lam WY., Wong KF., Tang NL., Tsang DN., Sung RY., Buckley TA., Tam JS., Cheng AF. 2001. Pathology of fatal human infection associated with avian influenza A H5N1 virus. *Journal of Medical Virology* 63:242–246.

To KKW., Hung IFN., Li IWS., Lee K-L., Koo C-K., Yan W-W., Liu R., Ho K-Y., Chu K-H., Watt C-L., Luk W-K., Lai K-Y., Chow F-L., Mok T., Buckley T., Chan JFW., Wong SSY., Zheng B., Chen H., Lau CCY., Tse H., Cheng VCC., Chan K-H., Yuen K-Y. 2010. Delayed clearance of viral load and marked cytokine activation in severe cases of pandemic H1N1 2009 influenza virus infection. *Clinical Infectious Diseases: An Official Publication of the Infectious Diseases Society of America* 50:850–859. DOI: 10.1086/650581.

Vemula SV., Zhao J., Liu J., Wang X., Biswas S., Hewlett I. 2016. Current Approaches for Diagnosis of Influenza Virus Infections in Humans. *Viruses* 8:96. DOI: 10.3390/v8040096.

Vidaña B., Martínez J., Martínez-Orellana P., García Migura L., Montoya M., Martorell J., Majó N. 2014. Heterogeneous pathological outcomes after experimental pH1N1 influenza infection in ferrets correlate with viral replication and host immune responses in the lung. *Veterinary Research* 45. DOI: 10.1186/s13567-014-0085-8.

Zou W., Chen D., Xiong M., Zhu J., Lin X., Wang L., Zhang J., Chen L., Zhang H., Chen H., Chen M., Jin M. 2013. Insights into the increasing virulence of the swine-origin pandemic H1N1/2009 influenza virus. *Scientific Reports* 3:1601. DOI: 10.1038/srep01601.

Zúñiga J., Torres M., Romo J., Torres D., Jiménez L., Ramírez G., Cruz A., Espinosa E., Herrera T., Buendía I., Ramírez-Venegas A., González Y., Bobadilla K., Hernández F., García J., Quiñones-Falconi F., Sada E., Manjarrez ME., Cabello C., Kawa S., Zlotnik A., Pardo A., Selman M. 2011. Inflammatory profiles in severe pneumonia associated with the pandemic influenza A/H1N1 virus isolated in Mexico City. *Autoimmunity* 44:562–570. DOI: 10.3109/08916934.2011.592885.

607
608

609 **Figure legends:**

610 ***Figure 1: Changes in body weight and lung viral load induced by A (H1N1) pdm09 virus.***

611 ***A)*** Average weight curve for C57BL6 mice infected through intranasal instillation with 50
612 µL CAT09 at 10^4 PFU A/Catalonia/63/2009 (H1N1pdm) and mock.

613 ***B)*** Viral load in lung homogenates collected at days 1, 5 and 10 pi. (n=6 for all groups).
614 Infection of Madin-Darby Canine Kidney cells was employed to measure viral titers.

615 The U Mann-Whitney test was used to compare weight loss and viral load between groups at
616 all sampling time. The significance level (α) was set at 0.05. Asterisks indicate significant
617 differences between groups (A) or between times points (B).

618

619 ***Figure 2: Histopathology of mice belonging to control and CAT09 groups at day 1, 5 and 10***
620 ***pi.***

621 A) Hematoxilin/Eosin stain. Arrows indicate the infiltrate in the viral infected lungs.

622 B) Microscopic lesional scores: grade 0 (no histopathological lesions observed), grade 1
623 (mild to moderate necrotising bronchiolitis), grade 2 (bronchointerstitial pneumonia
624 characterised by necrotising bronchiolitis and diffuse alveolar damage in adjacent
625 alveoli), and grade 3 (necrotising bronchiolitis and diffuse alveolar damage in the
626 majority of the pulmonary parenchyma) (Vidaña et al., 2014).

627

628 ***Figure 3: Pulmonary gene expression profiles at day 1, 5 and 10 post infection.***

629 A,B,C) Volcano plots for the representation of the number of genes with significant
630 variation of their expression levels between CAT09 and mock groups, at different time

points (1 (A), 5 (B) and 10 (C) dpi). The level of significance was fixed in $p < 0.05$, with Benjamini-Hochberg multiple testing corrections and Fold change ≥ 2. The list of genes differentially expressed between groups is shown in table S1.

D) *Top 20 Canonical signaling pathways altered by A (H1N1)pdm 09 virus.* The x-axis represents the percent of genes of eac*h pathway whose expression levels were altered by the virus. Genes i*nvolved in the top 20 canonical signalling pathways are shown in table S2.

E, F) Gene expression levels of cytokines, chemokines (E) and IFN-stimulated genes (F) during infection with A (H1N1) pdm09 influenza virus. The heat map depicts the most representative immune response-related genes (yellow and blue coloured genes in Table S3) that were differentially expressed between infection conditions at different time points. Colours represent the average value of gene expression levels of infected animals for each time point.

Table 1: Top 20 Canonical signaling pathways altered by A (H1N1)pdm 09 virus.

This table summarized the most significant canonical pathways identify by "Ingenuity pathway analysis". The IPA system implements Fisher's exact test to determine whether a canonical pathway is enriched with genes of interest (the level of significance was fixed in $p < 0.05$). The ratio shows the number of genes whose expression levels were different between CAT09 and mock groups, of the total of genes that have been described previously in each pathway.

654 ***Figure 4: Role of Hypercytokinemia/hyperchemokinemia in the Pathogenesis of Influenza***
655 ***signaling pathway.***
656 "Ingenuity pathway analysis" identified this route as the most altered pathway of the analysis.
657 Red: genes up-regulated in the infected group compared with non-infected mice.
658
659 ***Figure 5: Model of uncomplicated A (H1N1) pdm09 viral infection:***
660 The virus induced the activation of a marked pro-inflammatory program at the lung level
661 paralleling the emergence of histological changes. This program was associated to viral
662 clearance, and its resolution was accompanied by resolution of pneumonia.
663
664 **Supplemental information**:
665 ***Fig. S1: Droplet digital PCR validation of microarray data***: Expression values obtained from
666 the microarrays for IFNB1 and IL6 genes showed a significant positive correlation, confirmed by
667 using digital droplet PCR.
668
669 ***Table S1: List of genes differentially expressed between infected mice and controls.*** FC: fold
670 change. Highlighted genes in colour represent genes involved in the top 20 canonical pathways
671 identified by IPA. Orange: represent cytokines or chemokines genes and blue represent
672 interferon stimulated genes. Red represents granzyme molecules.
673
674 ***Fig. S2: Pulmonary gene expression profiles at day 5 and 10 post infection***
675 A) Venn diagram showing those genes whose expression levels differed from controls
676 either at day 5 and day 10, and those which differed only at one time point.

B) Heatmap of the common signature across different time points. The colour is proportional to their fold change (FC) compared to mock group, with the scale ranging from -4.2 FC (blue) to 4.2 FC (red).

Table S2: Genes involved in the top 20 canonical signalling pathways altered by A (H1N1) pdm 09 virus at day 5 post infection.

FC: fold change.

Table S3: Variation of gene expression along time in the infected group: Highlighted genes in colour represent genes involved in the top 20 canonical pathways identified by IPA. Orange: represent cytokines or chemokines genes and blue represent interferon stimulated genes. Red represents granzyme molecules.

Table S4: Studies evaluating host transcriptomic responses to A (H1N1) pdm09 influenza virus in animal models.

This table summarized the most significant previous studies evaluating the transcriptomic response to A (H1N1) pdm09 virus in different animal models.

EID_{50}: 50% Egg Infective Dose, $TCID_{50}$: 50% Tissue Culture Infective Dose, PFU: Plaque Forming Unit, dpi: days post infection.

Figure 1

Changes in body weight and lung viral load induced by A (H1N1) pdm09 virus.

A) Average weight curve for C57BL6 mice infected through intranasal instillation with 50 µL CAT09 at10 ^{4} PFU A/Catalonia/63/2009 (H1N1pdm) and mock.

B) Viral load in lung homogenates collected at days 1, 5 and 10 pi. (n = 6 for all groups). Infection of Madin-Darby Canine Kidney cells was employed to measure viral titers.

The U Mann-Whitney test was used to compare weight loss and viral load between groups at all sampling time. The significance level (α) was set at 0.05. Asterisks indicate significant differences between groups (A) or between times points (B).

*

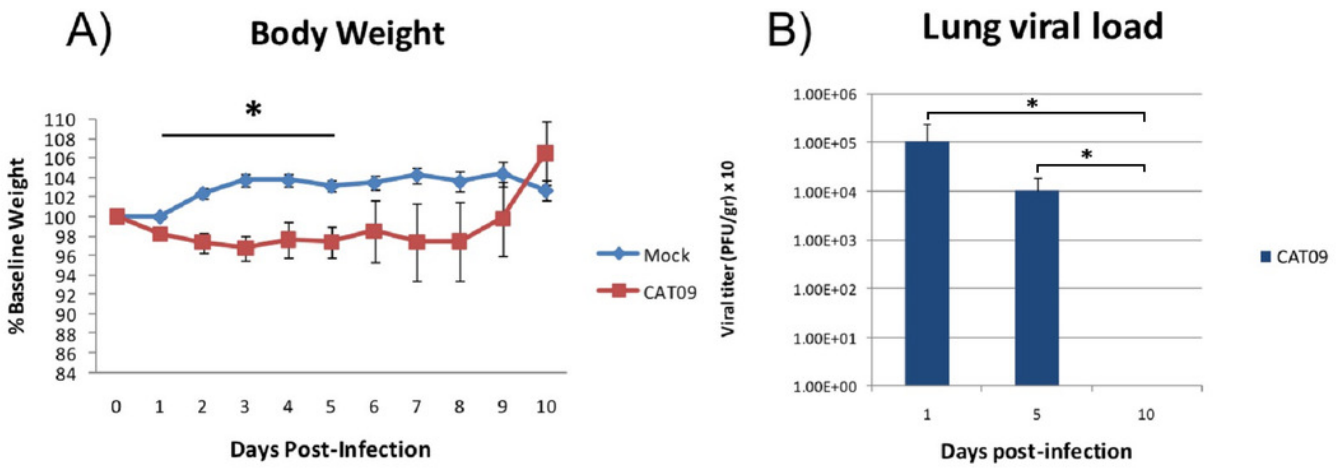

Figure 2

Histopathology of mice belonging to control and CAT09 groups at day 1, 5 and 10 pi.

A) Hematoxilin/Eosin stain. Arrows indicate the infiltrate in the viral infected lungs.

B) Microscopic lesional scores: grade 0 (no histopathological lesions observed), grade 1 (mild to moderate necrotising bronchiolitis), grade 2 (bronchointerstitial pneumonia characterised by necrotising bronchiolitis and diffuse alveolar damage in adjacent alveoli), and grade 3 (necrotising bronchiolitis and diffuse alveolar damage in the majority of the pulmonary parenchyma) (Vidaña et al., 2014) .

A)

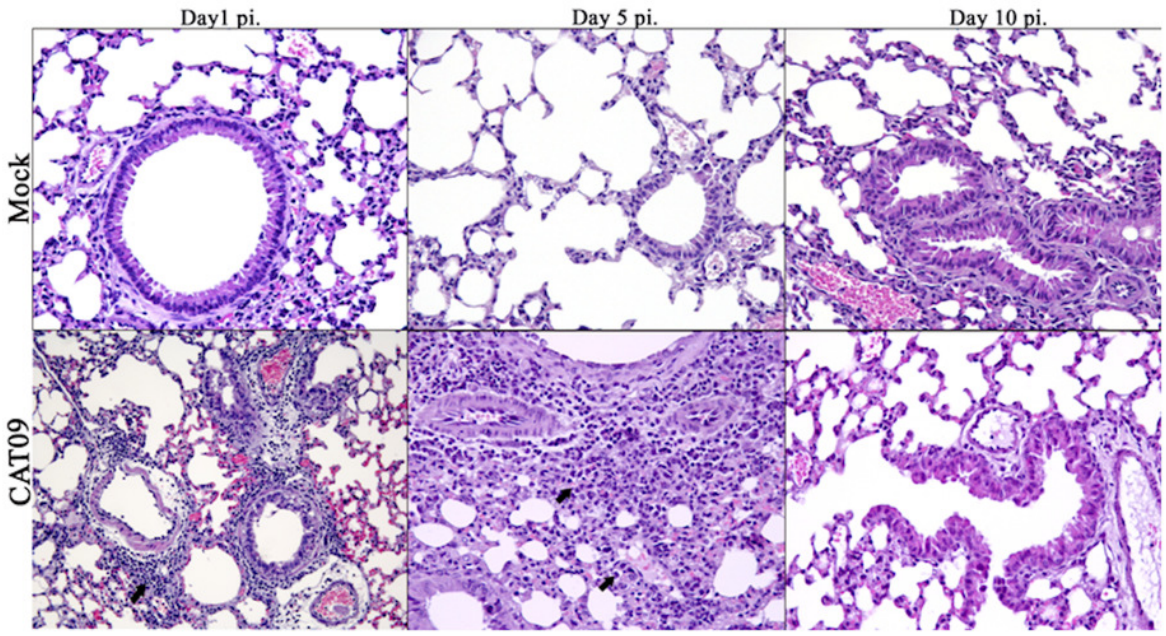

B)

	Experimental group	Hystological severity score				
		0	1	2	3	Average
Day 1pi.	Mock	6				0
	CAT09	3	2	1		0,7
Day 5pi.	Mock	6				0
	CAT09	1		5		1,7
Day 10 pi.	Mock	6				0
	CAT09	6				0

Figure 3

Pulmonary gene expression profiles at day 1, 5 and 10 post infection.

A,B,C) Volcano plots for the representation of the number of genes with significant variation of their expression levels between CAT09 and mock groups, at different time points (1 (A), 5 (B) and 10 (C) dpi). The level of significance was fixed in $p < 0.05$, with Benjamini-Hochberg multiple testing corrections and Fold change > 2. The list of genes differentially expressed between groups is shown in table S1.

D) *Top 20 Canonical signaling pathways altered by A (H1N1)pdm 09 virus.* The x-axis represents the percent of genes of eac*h pathway whose expression levels were altered by the virus. Genes i*nvolved in the top 20 canonical signalling pathways are shown in table S2.

E, F) Gene expression levels of cytokines, chemokines (E) and IFN-stimulated genes (F) during infection with A (H1N1) pdm09 influenza virus. The heat map depicts the most representative immune response-related genes (yellow and blue coloured genes in Table S3) that were differentially expressed between infection conditions at different time points. Colours represent the average value of gene expression levels of infected animals for each time point.

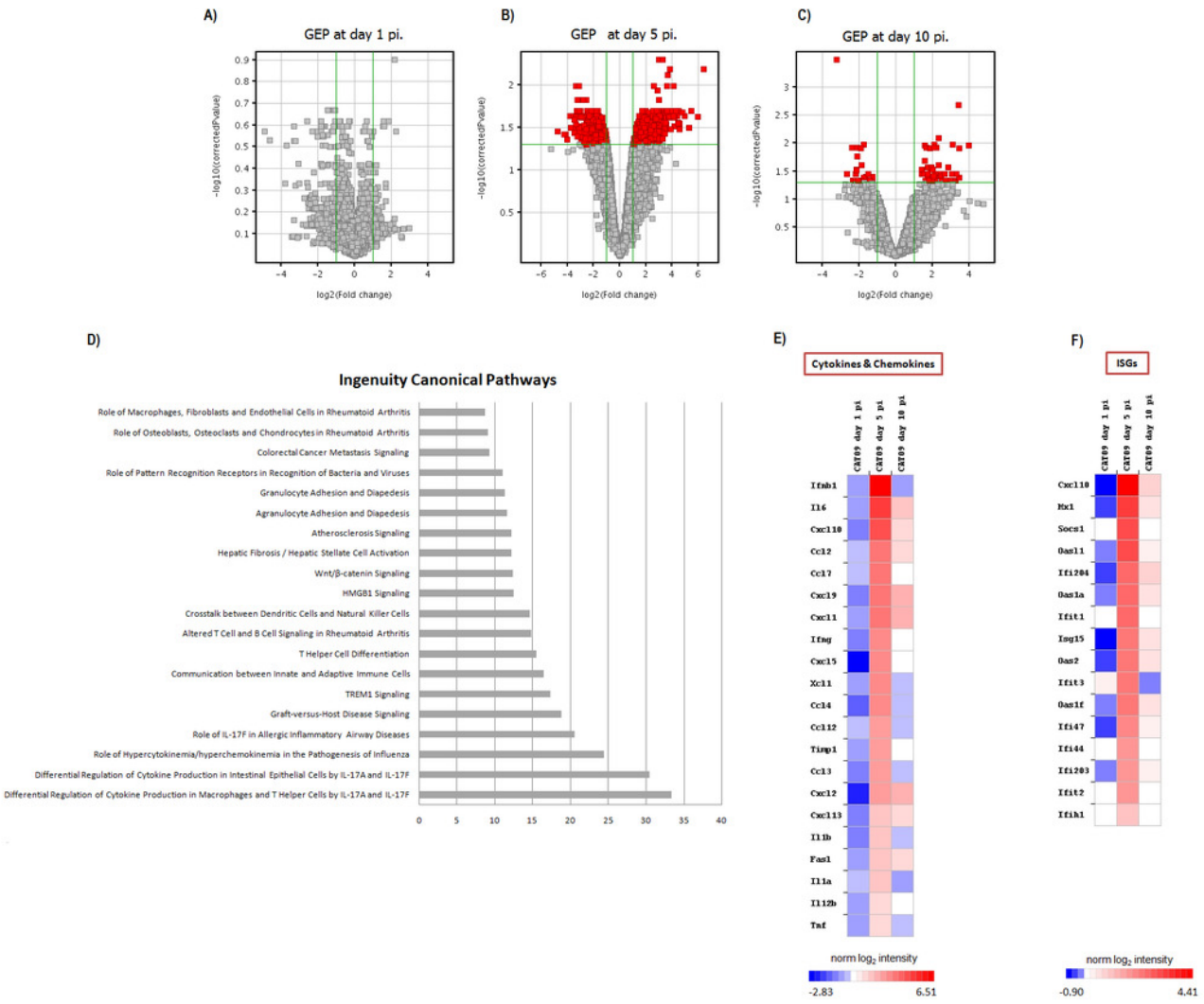
A)
GEP at day 1 pi.
-log10(correctedPvalue)
log2(Fold change)
B)
GEP at day 5 pi.
-log10(correctedPvalue)
log2(Fold change)
C)
GEP at day 10 pi.
-log10(correctedPvalue)
log2(Fold change)
D)
Ingenuity Canonical Pathways
Role of Macrophages, Fibroblasts and Endothelial Cells in Rheumatoid Arthritis
Role of Osteoblasts, Osteoclasts and Chondrocytes in Rheumatoid Arthritis
Colorectal Cancer Metastasis Signaling
Role of Pattern Recognition Receptors in Recognition of Bacteria and Viruses
Granulocyte Adhesion and Diapedesis
Agranulocyte Adhesion and Diapedesis
Atherosclerosis Signaling
Hepatic Fibrosis / Hepatic Stellate Cell Activation
Wnt/β-catenin Signaling
HMGB1 Signaling
Crosstalk between Dendritic Cells and Natural Killer Cells
Altered T Cell and B Cell Signaling in Rheumatoid Arthritis
T Helper Cell Differentiation
Communication between Innate and Adaptive Immune Cells
TREM1 Signaling
Graft-versus-Host Disease Signaling
Role of IL-17F in Allergic Inflammatory Airway Diseases
Role of Hypercytokinemia/hyperchemokinemia in the Pathogenesis of Influenza
Differential Regulation of Cytokine Production in Intestinal Epithelial Cells by IL-17A and IL-17F
Differential Regulation of Cytokine Production in Macrophages and T Helper Cells by IL-17A and IL-17F
E)
Cytokines & Chemokines
CRT09 day 1 pi
CRT09 day 5 pi
CRT09 day 10 pi
Ifnb1
Il6
Cxcl10
Ccl2
Ccl7
Cxcl9
Cxcl1
Ifng
Cxcl5
Xcl1
Ccl4
Ccl12
Timp1
Ccl3
Cxcl2
Cxcl13
Il1b
Fasl
Il1a
Il12b
Tnf
norm log2 intensity
-2.83
6.51
F)
ISGs
CRT09 day 1 pi
CRT09 day 5 pi
CRT09 day 10 pi
Cxcl10
Mx1
Socs1
Oasl1
Ifi204
Oasla
Ifit1
Isg15
Oas2
Ifit3
Oasl1f
Ifi47
Ifi44
Ifi203
Ifit2
Ifih1
norm log2 intensity
-0.90
4.41

Figure 4

Role of Hypercytokinemia/hyperchemokinemia in the Pathogenesis of Influenza signaling pathway.

“Ingenuity pathway analysis” identified this route as the most altered pathway of the analysis. Red: genes up-regulated in the infected group compared with non-infected mice.

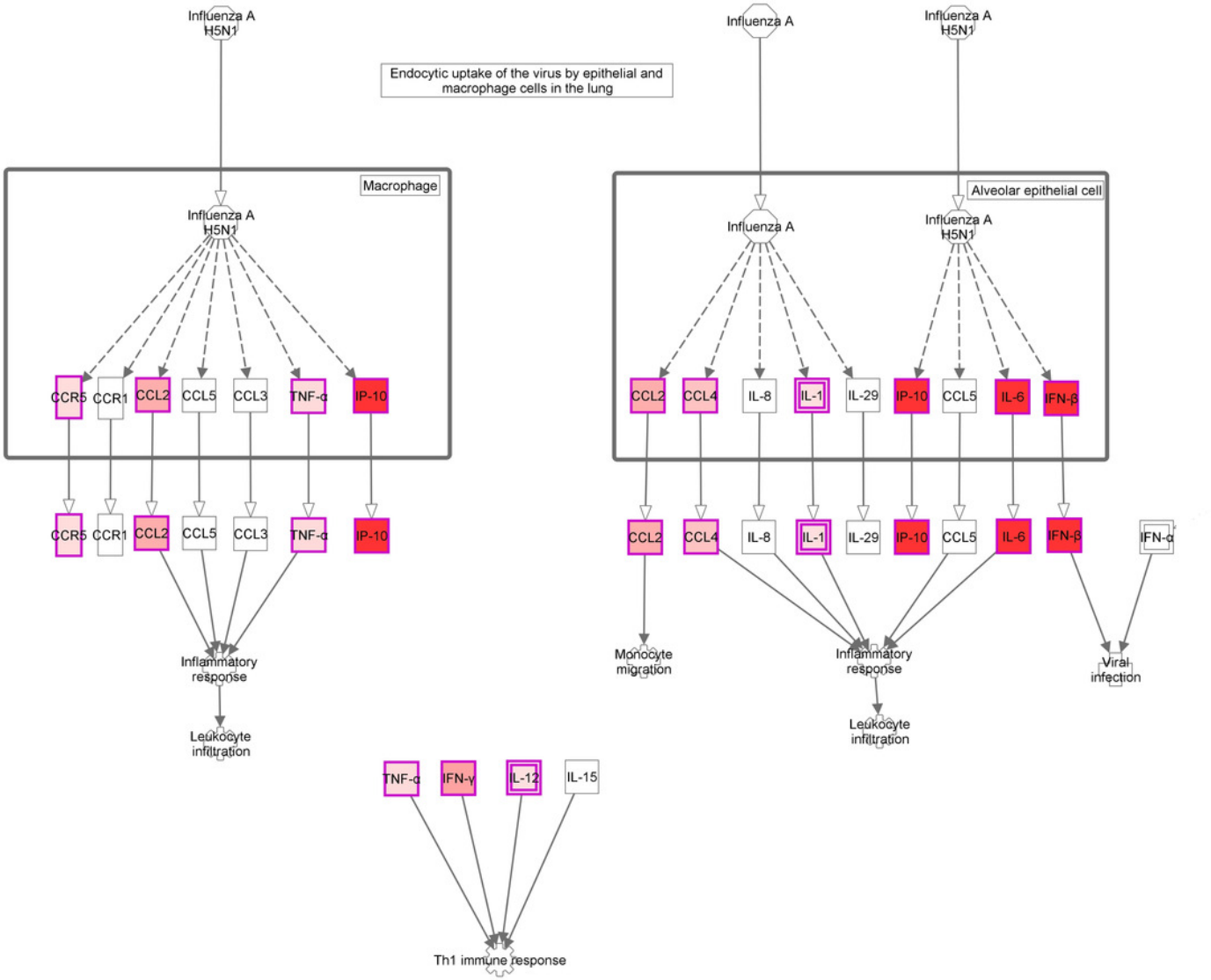

Figure 5

Model of uncomplicated A (H1N1) pdm09 viral infection

The virus induced the activation of a marked pro-inflammatory program at the lung level paralleling the emergence of histological changes. This program was associated to viral clearance, and its resolution was accompanied by resolution of pneumonia.

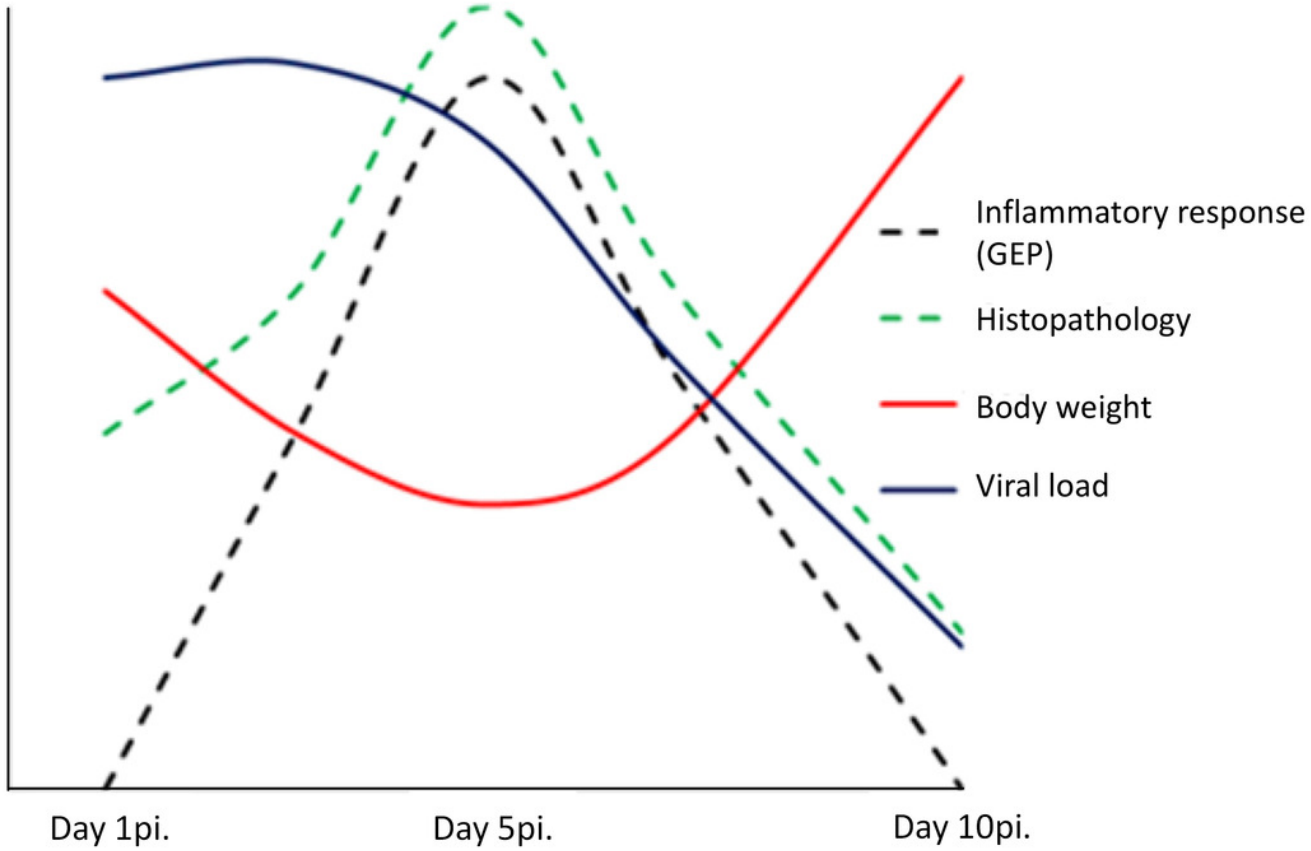

Table 1(on next page)

Top 20 Canonical signaling pathways altered by A (H1N1)pdm 09 virus.

This table summarized the most significant canonical pathways identify by “Ingenuity pathway analysis”. The IPA system implements Fisher's exact test to determine whether a canonical pathway is enriched with genes of interest (the level of significance was fixed in $p < 0.05$). The ratio show the number of genes whose expression levels were different between CAT09 and mock groups, of the total of genes that have been described previously in each pathway.

1 ***Top 20 Canonical signaling pathways altered by A (H1N1)pdm 09 virus***

Ingenuity Canonical Pathways	*p value*	Ratio	Top Functions & Diseases
Role of Hypercytokinemia/hyperchemokinemia in the Pathogenesis of Influenza	<0.001	0.244	Cell-To-Cell Signaling and Interaction; Cellular Movement; Hematological System Development and Function
Hepatic Fibrosis / Hepatic Stellate Cell Activation	<0.001	0.122	Organismal Injury and Abnormalities; Cardiovascular System Development and Function; Organismal Development
Communication between Innate and Adaptive Immune Cells	<0.001	0.165	Cell-To-Cell Signaling and Interaction; Cellular Growth and Proliferation; Hematological System Development and Function
Wnt/β-catenin Signaling	<0.001	0.124	Gene Expression; Cellular Development; Tissue Development
Agranulocyte Adhesion and Diapedesis	<0.001	0.116	Cell-To-Cell Signaling and Interaction; Tissue Development; Hematological System Development and Function
TREM1 Signaling	<0.001	0.173	Cell-To-Cell Signaling and Interaction; Hematological System Development and Function; Immune Cell Trafficking
Differential Regulation of Cytokine Production in Intestinal Epithelial Cells by IL-17A and IL-17F	<0.001	0.304	Cell-To-Cell Signaling and Interaction; Hematological System Development and Function; Immune Cell Trafficking
Granulocyte Adhesion and Diapedesis	<0.001	0.113	Cell-To-Cell Signaling and Interaction; Hematological System Development and Function; Immune Cell Trafficking
Altered T Cell and B Cell Signaling in Rheumatoid Arthritis	<0.001	0.148	Hematological System Development and Function; Tissue Morphology; Cellular Development
Differential Regulation of Cytokine Production in Macrophages and T Helper Cells by IL-17A and IL-17F	<0.001	0.333	Cell-To-Cell Signaling and Interaction; Hematological System Development and Function; Immune Cell Trafficking
Role of IL-17F in Allergic Inflammatory Airway Diseases	<0.001	0.205	Connective Tissue Disorders; Immunological Disease; Inflammatory Disease
Crosstalk between Dendritic Cells and Natural Killer Cells	<0.001	0.146	Cell-To-Cell Signaling and Interaction; Cellular Growth and Proliferation; Hematological System Development and Function
HMGB1 Signaling	<0.001	0.125	Cell-To-Cell Signaling and Interaction; Cellular Movement; Hematological System Development and Function
Graft-versus-Host Disease Signaling	<0.001	0.188	Cellular Immune Response; Disease-Specific Pathways
T Helper Cell Differentiation	<0.001	0.155	Cell-mediated Immune Response; Cellular Development; Cellular Function and Maintenance
Atherosclerosis Signaling	<0.001	0.122	Cell-To-Cell Signaling and Interaction; Cellular Movement; Hematological System Development and Function
Role of Macrophages, Fibroblasts and Endothelial Cells in Rheumatoid Arthritis	<0.001	0.087	Cell Death and Survival; Cellular Development; Cellular Growth and Proliferation
Colorectal Cancer Metastasis Signaling	<0.001	0.093	Cell Death and Survival; Cell Cycle; Cellular Development
Role of Osteoblasts, Osteoclasts and Chondrocytes in Rheumatoid Arthritis	0.001	0.091	Hematological System Development and Function; Tissue Morphology; Cellular Development
Role of Pattern Recognition Receptors in Recognition of Bacteria and Viruses	0.001	0.110	Antimicrobial Response; Inflammatory Response; Infectious Disease